Porphyrin Aggregation

DOI: 10.1002/ange.201000162

Dilution-Induced Self-Assembly of Porphyrin Aggregates: A Consequence of Coupled Equilibria**

Floris Helmich, Cameron C. Lee, Marko M. L. Nieuwenhuizen, Jeroen C. Gielen, Peter C. M. Christianen, Antje Larsen, George Fytas, Philippe E. L. G. Leclère, Albertus P. H. J. Schenning, and E. W. Meijer**

The self-assembly of organic molecules has attracted substantial interest as a bottom-up approach to create nano-sized objects. Their properties depend strongly on the design, arrangement, and number of molecules in the aggregate. For supramolecular polymers, the monomers are entirely held together by non-covalent interactions; these interactions are typically weak, reversible, and highly sensitive to variables such as temperature, concentration, and solvent polarity.[1,2] These variables have often been employed as tools to control the self-assembly process, but other relatively new methods like templating[3] and end-capping[4] have also been described. For these responsive systems, an understanding of the self-assembly mechanism is a crucial aspect, as different molar distributions over monomers and aggregates are obtained in case of isodesmic or cooperative systems.[2] In the latter, the self-assembly is described by two distinct association constants yielding a bimodal distribution of monomers and extended aggregates.[5]

Herein, we present the employment of pyridine as an axial ligand to influence the cooperative self-assembly of zinc porphyrins. We show that pyridine specifically coordinates to porphyrin monomers that coexist with long, one-dimensional aggregates, leading to a system with coupled equilibria that shows extraordinary behavior. At a critical pyridine concentration, a sharp transition to a completely depolymerized state is observed, which then reassembes upon dilution until the critical aggregation concentration is reached. To fully verify these observations with re-entrant phase transitions, it is a prerequisite to investigate the cooperative nature of the porphyrin self-assembly without and with pyridine.

Porphyrin **1** is based on a symmetrical amide-substituted discotic with chiral hydrocarbon side chains (Scheme 1). The design is inspired by self-assembling porphyrins with similar functionalization patterns that provide one-dimensional aggregates in apolar organic solvents.[6] Compound **1** is synthesized from commercially available *meso*-tetrakis-(4-carboxyphenyl)porphyrin and a chiral trialkoxy aniline wedge.[7] After amidation, zinc insertion, column chromatography, and recycling size-exclusion chromatography, porphyrin **1** was obtained in 71% yield and fully characterized.[7]

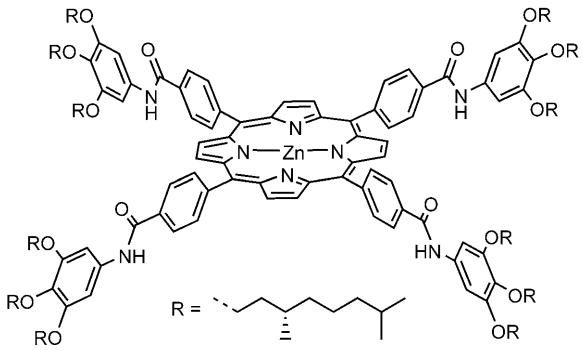

Scheme 1. Chiral amide-functionalized zinc tetraphenylporphyrin **1**.

At room temperature, **1** is molecularly dissolved in chloroform, and it has a sharp Soret band at $\lambda_{max} = 422$ nm. In methylcyclohexane (MCH), a large blue-shift to a broadened band at $\lambda_{max} = 390$ nm is observed, which exists even at sub-micromolar concentrations.[7] This aggregate band, which is typically observed for cofacially arranged porphyrins,[8] shows an intense bisignate Cotton effect in the circular dichroism (CD) spectrum, indicating a helical arrangement of the chromophores in the aggregate. Solution-based IR spectroscopy in MCH shows a shift of the amide C=O

[*] F. Helmich, Dr. C. C. Lee, M. M. L. Nieuwenhuizen, Dr. A. P. H. J. Schenning, Prof. Dr. E. W. Meijer
Laboratory of Macromolecular and Organic Chemistry
Institute for Complex Molecular Systems
Eindhoven University of Technology
P.O. Box 513, 5600 MB Eindhoven (The Netherlands)
Fax: (+31) 40-245-1036
E-mail: a.p.h.j.schenning@tue.nl
e.w.meijer@tue.nl

J. C. Gielen, Dr. P. C. M. Christianen
Institute for Molecules and Materials
Radboud University Nijmegen
Toernooiveld 7, 6525 ED Nijmegen (The Netherlands)

A. Larsen, Prof. G. Fytas
Department of Material Science, F.O.R.T.H./I.E.S.L.
P.O. Box 1527, 71110 Heraklion (Greece)

Dr. P. E. L. G. Leclère
Laboratory for Chemistry of Novel Materials
Université de Mons, 7000 Mons (Belgium)

[**] This work was supported by the Council of Chemical Sciences of the Netherlands Organization for Scientific Research (CW-NWO). P.E.L.G.L. is Research Associate from FRS-FNRS (Belgium). We would like to thank Maarten Smulders and Tom de Greef for stimulating discussions, Tania Larsen for early contributions to the project, and Prof. Alison Rodger and Dr. Matthew Hicks for assisting with flow linear dichroism experiments.

Supporting information for this article is available on the WWW under http://dx.doi.org/10.1002/anie.201000162.

stretching band to lower wave numbers relative to chloroform, indicating intermolecular hydrogen bonding.[7]

The porphyrin assemblies are disrupted by heating, as evidenced by a red-shifted Soret band at 419 nm and a disappearance of the CD response. Upon cooling at a concentration of 5.0×10^{-5} mol L^{-1}, an apparent isosbestic transition from 419 to 390 nm is observed with a reappearance of the CD effect at 69 °C (Figure 1).[9] By probing the absorbance at 390 nm, a non-sigmoidal cooling curve is observed with a sharp transition at 69 °C (Figure 1, inset), which indicates a highly cooperative self-assembly process.[10] To determine the thermodynamic parameters, we fitted the cooling curve with a temperature-dependent nucleation–elongation model, from which we estimate an enthalpy release of 110 kJ mol^{-1} and a high degree of cooperativity (K_a) of 5×10^{-5}.[11]

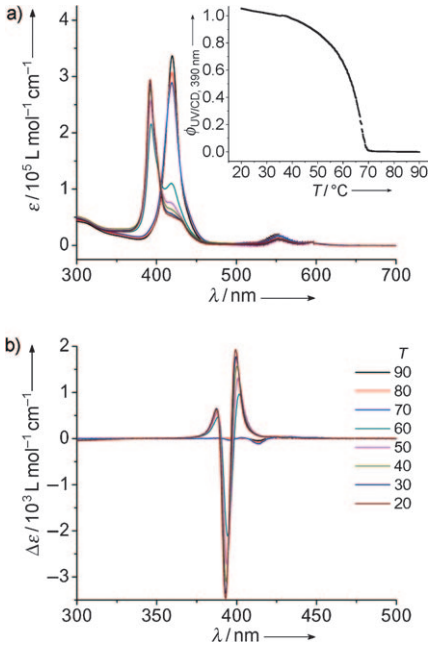

Figure 1. Temperature-dependent a) UV/Vis and b) CD spectrum of **1** in methylcyclohexane between 20 and 90 °C with 10 °C intervals. Inset in (a) shows a −1 °C min^{-1} cooling curve probed at 390 nm. [**1**] = 5.0×10^{-5} mol L^{-1}.

AFM studies of a drop-cast solution of **1** on HOPG show micrometer-long curled fibrillar nanostructures with a typical height of 3 nm, which perfectly matches edge-on stacking of **1** into single fibers onto the surface (Figure 2a). In solution, static and multi-angle dynamic light-scattering measurements performed on a 6.6×10^{-5} mol L^{-1} solution of **1** in MCH indicate rod-like aggregates with a persistence length of 100 nm.[7] Consistent with these results, concentrated solutions of **1** are highly viscous, and the aggregates undergo facile alignment when placed under flow in a Couette cell or when placed in a magnetic field (Figure 2b).[7,12]

After elucidation of the self-assembly without pyridine, the addition of the axial ligand to aggregates of **1** was studied at room temperature. At 1.2×10^{-5} mol L^{-1}, two distinct transitions are observed upon the addition of pyridine

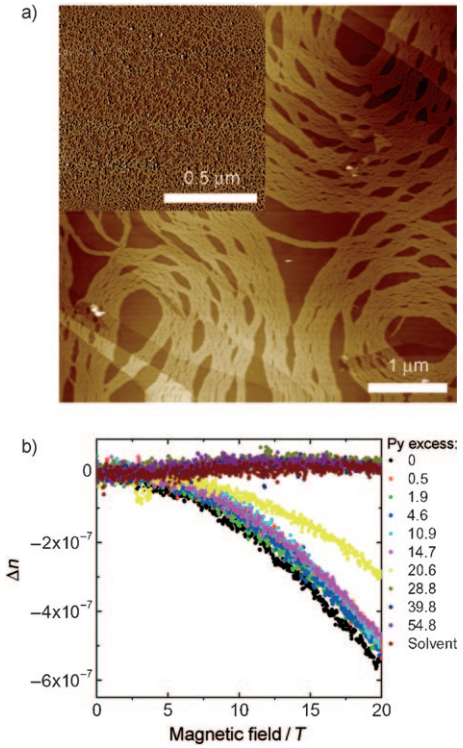

Figure 2. a) AFM height image of **1** deposited from methylcyclohexane on HOPG. Inset: AFM of **1** deposited from same solution with 500 equivalents of pyridine. b) Birefringence $\Delta n = n_{perp} - n_{par}$ induced by a magnetic field for **1** upon pyridine addition in methylcyclohexane at room temperature. [**1**] = 5.0×10^{-5} mol L^{-1}.

(Figure 3a).[13] Without pyridine, the porphyrin Soret band appears at 390 nm. When 40 equivalents of pyridine are added, a new red-shifted and split band at 418 and 427 nm appears. The exciton splitting energy of 500 cm^{-1} is indicative for a dimeric porphyrin–pyridine adduct.[14] This proposal is strengthened by the presence of a weak CD spectrum in the exciton split band region.[7] Ultimately, at a pyridine excess of 80000, this split Soret band gradually converts into a single, narrow, CD-silent band at 430 nm. This band is identical in shape and position to a monomeric porphyrin–pyridine adduct,[13] which suggests that at this rather high pyridine concentration, the dimeric adducts have dissociated owing to the increased solvent polarity, breaking up the hydrogen bonds within the dimer. The full titration curve spanning the aggregated state (390 nm) and the dimeric pyridine-complexed state (427 nm) shows a sharp transition when either band is probed (Figure 3b).

As a similar behavior is not observed for the free-base derivative of **1**,[7] the titration data suggest that axial ligation is responsible for depolymerization. Indeed, the spectral changes at 390 and 427 nm in the UV/Vis spectra are accompanied by a disappearance of the CD effect and a sharp drop in solution viscosity.[7] Moreover, it is observed that no fibrillar structures are observed in the AFM image (Figure 2a, inset), the porphyrins no longer align in a magnetic field (Figure 2b), and low-light scattering intensities confirm the presence of small adducts.[7]

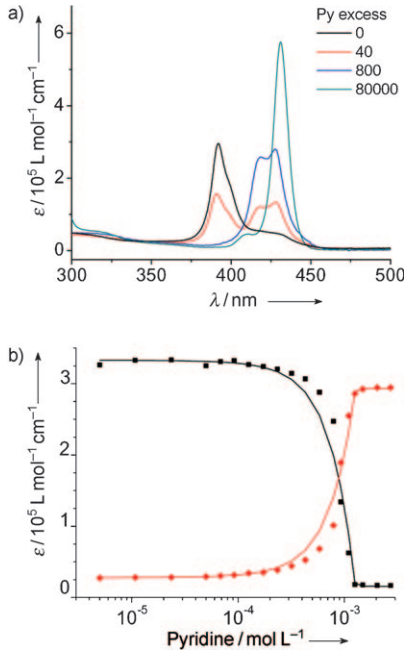

Figure 3. a) UV/Vis spectra of porphyrin aggregates in methylcyclohexane at room temperature, with 0, 40, 800, and 80000 equivalents of pyridine corresponding to aggregates, aggregates and pyridine-complexed dimers, pyridine-complexed dimers, and pyridine-complexed monomers, respectively. b) Corresponding pyridine titration curves probed at the aggregate band (390 nm, black) and the pyridine-complexed dimer band (427 nm, red). Symbols represent data points, and lines are best-fit curves. [**1**] = 1.2×10^{-5} mol L^{-1}.

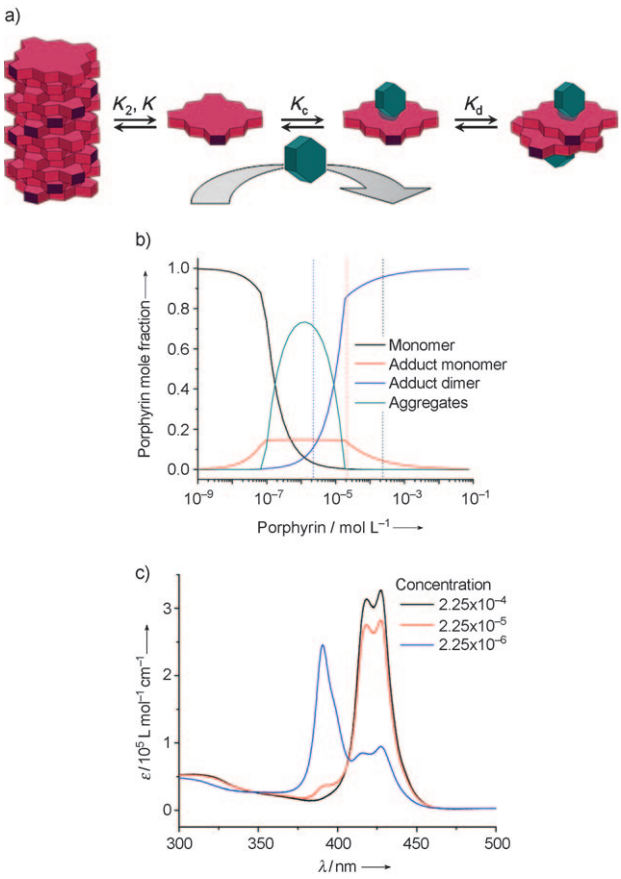

Figure 4. a) A model in which aggregates, monomers, and monomeric and dimeric porphyrin–pyridine adducts are connected by equilibrium constants. b) Model simulation with the data obtained from curve fitting at a fixed pyridine excess of 40 equivalents; $K_2 = 685$ L mol^{-1}, $K = 1.37\times10^7$ L mol^{-1}, $K_c = 5.1\times10^4$ L mol^{-1}, and $K_d = 1.1\times10^6$ L mol^{-1}. c) Dilution-induced self-assembly of **1** in MCH at a fixed pyridine excess of 40 probed over three orders of magnitude in concentration at room temperature.

To interpret the shape of the titration curves observed, we fitted this pyridine titration using experimentally determined molar absorptivities and equilibrium constants for the porphyrin aggregates and porphyrin–pyridine adducts, systematically ruling out a variety of different depolymerization mechanisms based on the quality of the fits obtained.[7] We have found that the best fits are obtained for a model that includes 1) cooperative self-assembly of the porphyrins, 2) the formation of one-to-one adducts between monomers of **1** and pyridine, and 3) the dimerization of these adducts (Figure 4a).[15] Given the extremely low concentration of monomers expected for this system ($<10^{-7}$ mol L^{-1}), it is remarkable that monomers are involved in the equilibrium at all. However, the statistic effect caused by the cooperative self-assembly, in which the number of binding sites provided by monomers is relatively high compared to that number provided by aggregate end groups, could be the driving force towards axial ligation of predominantly monomers.[5,16] Another aspect we would encounter is an affinity difference of the axial ligand towards monomers and aggregates where enhanced π–π interactions reduce the affinity of the zinc for the Lewis base.[17]

With absorbance data as output of the model, we performed simultaneous nonlinear curve-fitting on the pyridine titration data of the aggregate and the pyridine-complexed dimer at 390 and 427 nm, respectively (Figure 3b). In the full model, the absorbance at a given wavelength is determined by eight parameters: four equilibrium constants and four extinction coefficients. To avoid the necessity to fit all eight parameters from one dataset, we obtained most of the parameters from separate experiments. The equilibrium constants describing the cooperative self-assembly of **1** (K_2 and K) are derived from the aforementioned temperature-dependent nucleation–elongation model[18] and the value for K_c from a control experiment.[13] These measurements also provide the extinction coefficients, so the only parameters left for fitting are the dimerization constant (K_d) and the extinction coefficient of the pyridine-complexed dimer. A dimerization constant of $K_d = 1.1\times10^6$ L mol^{-1} is obtained, which approximates the value of the elongation constant (K).

With all model parameters available, we are able to simulate the behavior of the system at different conditions. At a fixed pyridine-to-porphyrin ratio of 40, a strong effect on the distribution of **1** over the four components is observed when the total concentration is changed (Figure 4b). At low concentrations, monomers of **1** do not interact with either pyridine or themselves. At the critical aggregation concentration (ca. 10^{-7} mol L^{-1}), the pyridine interaction is insufficient to avoid porphyrin self-assembly, yet at about

10^{-6} mol L^{-1}, pyridine complexation hampers aggregation by the formation of dimers. Because of the high dimerization constant, pyridine-complexed dimers are formed exclusively, thus resulting in a low abundance of pyridine-complexed monomers. The same holds for free monomers that are involved in the cooperative self-assembly, so in the presence of pyridine, either aggregates or pyridine-complexed dimers are the most abundant species.

The simulation shows that upon dilution from 10^{-4} to 10^{-6} mol L^{-1}, the depolymerized state becomes unfavorable and aggregation is enhanced. To verify this re-entrant phase transition, we performed dilution experiments at a fixed pyridine-to-porphyrin ratio of 40. In the same concentration window, an almost full transition from the dimeric pyridine-complexed state to the aggregated state is obtained over two orders of magnitude in concentration (Figure 4c). This dilution-induced self-assembly is unusual for supramolecular polymers and it arises in multi-component systems in which an additional component affects the cooperative self-assembly by an orthogonal interaction with the main component. Similar behavior is found in protein systems in which protein unfolding takes place upon the addition of denaturant, and renaturation occurs upon dilution albeit the mechanism is different.[19]

In conclusion, with this class of zinc-porphyrin-based supramolecular polymers, we can bias the self-assembly process with the additional tool of molecular recognition by axial ligation of a Lewis base. Remarkably, driven by the highly cooperative self-assembly, monomers possess a prime role in the depolymerization mechanism. Our results showed that a multi-component system with coupled equilibria leads to the dilution-induced self-assembly property, which is in agreement with model predictions. With these findings, we envision that the approach of systems chemistry provides new tools in controlling molecular self-assembly and the development of new stimuli-responsive materials.[20]

Received: January 11, 2010
Published online: April 8, 2010

Keywords: aggregation · porphyrins · self-assembly · solvent effects · systems chemistry

[1] J. M. Lehn, *Supramolecular Chemistry: Concepts and Perspectives*, Wiley-VCH, Weinheim, **1995**.
[2] T. F. A. De Greef, M. M. J. Smulders, M. Wolffs, A. P. H. J. Schenning, R. P. Sijbesma, E. W. Meijer, *Chem. Rev.* **2009**, *109*, 5687.
[3] P. G. A. Janssen, S. Jabbari-Farouji, M. Surin, X. Vila, J. C. Gielen, T. F. A. de Greef, M. R. J. Vos, P. H. H. Bomans, N. Sommerdijk, P. C. M. Christianen, P. E. L. G. Leclère, R. Lazzaroni, P. van der Schoot, E. W. Meijer, A. P. H. J. Schenning, *J. Am. Chem. Soc.* **2009**, *131*, 1222.
[4] a) D. Furutsu, A. Satake, Y. Kobuke, *Inorg. Chem.* **2005**, *44*, 4460; b) R. P. Sijbesma, F. H. Beijer, L. Brunsveld, B. J. B. Folmer, J. Hirschberg, R. F. M. Lange, J. K. L. Lowe, E. W. Meijer, *Science* **1997**, *278*, 1601.
[5] a) D. H. Zhao, J. S. Moore, *Org. Biomol. Chem.* **2003**, *1*, 3471; b) D. H. Zhao, J. S. Moore, *J. Am. Chem. Soc.* **2003**, *125*, 16294.
[6] a) J. Z. Li, H. Xin, M. Li, *Liq. Cryst.* **2006**, *33*, 913; b) S. W. Kang, Q. Li, B. D. Chapman, R. Pindak, J. O. Cross, L. F. Li, M. Nakata, S. Kumar, *Chem. Mater.* **2007**, *19*, 5657; c) M. Shirakawa, S. Kawano, N. Fujita, K. Sada, S. Shinkai, *J. Org. Chem.* **2003**, *68*, 5037; d) M. Shirakawa, N. Fujita, S. Shinkai, *J. Am. Chem. Soc.* **2005**, *127*, 4164; e) T. Kishida, N. Fujita, K. Sada, S. Shinkai, *Langmuir* **2005**, *21*, 9432; f) F. J. M. Hoeben, M. Wolffs, J. Zhang, S. De Feyter, P. E. L. G. Leclère, A. P. H. J. Schenning, E. W. Meijer, *J. Am. Chem. Soc.* **2007**, *129*, 9819.
[7] See the Supporting Information.
[8] N. C. Maiti, S. Mazumdar, N. Periasamy, *J. Phys. Chem. B* **1998**, *102*, 1528.
[9] Prior to the 30 nm blue-shift, the monomer band slightly broadens, which is probably due to the formation of an intermediate state that is weakly CD-active in the monomer absorbance range.
[10] In the cooling curve, ϕ represents the normalized fraction of aggregated species. A similar cooling curve is observed when monitoring the CD intensity, suggesting that the formation of helical aggregates coincides just after nucleation. Upon further cooling from T_e, the aggregate band shows a slight blue-shift; causing a small difference in the elongation regime of the cooling curve probed either by CD or UV/Vis spectroscopy.
[11] M. M. J. Smulders, A. P. H. J. Schenning, E. W. Meijer, *J. Am. Chem. Soc.* **2008**, *130*, 606.
[12] I. O. Shklyarevskiy, P. Jonkheijm, N. Stutzmann, D. Wasserberg, H. J. Wondergem, P. C. M. Christianen, A. P. H. J. Schenning, D. M. de Leeuw, Z. Tomovic, J. S. Wu, K. Müllen, J. C. Maan, *J. Am. Chem. Soc.* **2005**, *127*, 16233.
[13] The association constant and spectral changes of **1** with pyridine were determined in chloroform, and showed a red-shift of the Soret band from 422 to 432 nm ($K_{CHCl_3} = 1.2 \times 10^4$ L mol^{-1}). In MCH, the addition of pyridine to an *N*-methylated analogue **1**,[7] which is molecularly dissolved in this solvent, shows a red-shift from 419 to 429 nm and a five-fold higher association constant ($K_c = 5.1 \times 10^4$ L mol^{-1}).[7]
[14] V. V. Borovkov, J. M. Lintuluoto, Y. Inoue, *J. Phys. Chem. B* **1999**, *103*, 5151.
[15] Possible two-fold coordination of pyridine to the Zn^{2+}-ions is not expected to be significant in the concentration range of the titration and is not included in the model, which also does not describe the dissociation of pyridine-complexed dimers owing to polarity.
[16] At a concentration of 1.2×10^{-5} mol L^{-1}, 85% of the binding sites is provided by monomers.[7]
[17] C. A. Hunter, P. Leighton, J. K. M. Sanders, *J. Chem. Soc. Perkin Trans. 1* **1989**, 547.
[18] The parameters for the concentration-dependent K_2K model are adapted from the parameters obtained from the temperature-dependent model: M. M. J. Smulders, M. M. L. Nieuwenhuizen, T. F. A. de Greef, P. van der Schoot, A. P. H. J. Schenning, E. W. Meijer, *Chem. Eur. J.* **2010**, *16*, 362.[7]
[19] a) J. M. Berg, J. L. Tymoczko, L. Stryer, *Biochemistry*, W. H. Freeman, San Francisco, **2002**; b) T. M. Hermans, M. A. C. Broeren, N. Gomopoulos, P. van der Schoot, M. H. P. van Genderen, N. Sommerdijk, G. Fytas, E. W. Meijer, *Nat. Nanotechnol.* **2009**, *4*, 721.
[20] R. F. Ludlow, S. Otto, *Chem. Soc. Rev.* **2008**, *37*, 101.

